



Invited paper

Recurring types of variability and transitions in the ~620 kyr record of climate change from the Chew Bahir basin, southern Ethiopia

Martin H. Trauth^{a,*}, Asfawossen Asrat^b, Andrew S. Cohen^c, Walter Duesing^a, Verena Foerster^d, Stefanie Kaboth-Bahr^a, K. Hauke Kraemer^{a,e}, Henry F. Lamb^f, Norbert Marwan^e, Mark A. Maslin^g, Frank Schäbitz^d

^a University of Potsdam, Institute of Geosciences, Potsdam, Germany

^b Addis Ababa University, School of Earth Sciences, Addis Ababa, Ethiopia

^c University of Arizona, Department of Geosciences, Tucson, USA

^d University of Cologne, Institute of Geography Education, Cologne, Germany

^e Potsdam Institute for Climate Impact Research, Potsdam, Germany

^f Aberystwyth University, Department of Geography and Earth Sciences, Aberystwyth, UK

^g University College London, Geography Department, London, UK

ARTICLE INFO

Article history:

Received 3 August 2020

Received in revised form

17 December 2020

Accepted 18 December 2020

Available online 10 June 2021

Handling Editor: A. Voelker

Keywords:

Recurrence plots

Paleoclimate dynamics

Eastern africa

Homo sapiens

ABSTRACT

The Chew Bahir Drilling Project (CBDP) aims to test possible linkages between climate and hominin evolution in Africa through the analysis of sediment cores that have recorded environmental changes in the Chew Bahir basin (CHB). In this statistical project we used recurrence plots (RPs) together with a recurrence quantification analysis (RQA) to distinguish two types of variability and transitions in the Chew Bahir aridity record and compare them with the ODP Site 967 wetness index from the eastern Mediterranean. The first type of variability is one of slow variations with cycles of ~20 kyr, reminiscent of the Earth's precession cycle, and subharmonics of this orbital cycle. In addition to these cyclical wet-dry fluctuations in the area, extreme events often occur, i.e. short wet or dry episodes, lasting for several centuries or even millennia, and rapid transitions between these wet and dry episodes. The second type of variability is characterized by relatively low variation on orbital time scales, but significant century-millennium-scale variations with progressively increasing frequencies. Within this type of variability there are extremely fast transitions between dry and wet within a few decades or years, in contrast to those within Type 1 with transitions over several hundreds of years. Type 1 variability probably reflects the influence of precessional forcing in the lower latitudes at times with maximum values of the long (400 kyr) eccentricity cycle of the Earth's orbit around the sun, with the tendency towards extreme events. Type 2 variability seems to be linked with minimum values of this cycle. There does not seem to be a systematic correlation between Type 1 or Type 2 variability with atmospheric CO₂ concentration. The different types of variability and the transitions between those types had important effects on the availability of water, and could have transformed eastern Africa's environment considerably, which would have had important implications for the shaping of the habitat of *H. sapiens* and the direct ancestors of this species.

© 2020 Elsevier Ltd. All rights reserved.

1. Introduction

Some hypotheses about the relationship of climate and human evolution suggest that episodes of increased climate variability (e.g. Potts, 1996, 2013; Maslin and Trauth, 2009) or prominent

transitions (e.g. Vrba, 1985, 1993, 1995) may have enhanced rates of speciation, dispersal and technological innovation. Examples on long time scales are the termination of the permanent El Niño and the establishment of the modern Walker/Hadley circulation between 3.5 and 2.0 Ma, possibly linked to the closure of the Indonesian sea way (Cane and Molnar, 2001; Ravelo et al., 2004; Trauth et al., 2009), and the intensification of the Northern Hemisphere Glaciation at 2.75 Ma (e.g., Trauth et al., 2009; Bonnefille, 2010),

* Corresponding author.

E-mail address: trauth@uni-potsdam.de (M.H. Trauth).

both being subject to lively discussions during the last four decades (Vrba, 1985, 1993, 1995; deMenocal, 1995, 2004; Brovkin and Claussen, 2008; Kröpelin et al., 2008a,b; Trauth et al., 2005, 2009). As the most recent example of a major climate shift in the tropics, in particular in Africa, the termination of the African Humid Period (AHP, ~15–5 kyr BP) has also been intensely investigated, in particular the extent to which it was abrupt or gradual (deMenocal et al., 2000; Kuper and Kröpelin, 2006; Tierney and deMenocal, 2013; Trauth et al., 2018), which is important for potential migration scenarios within and across the Sahara and cultural transformations (Kuper and Kröpelin, 2006).

Revived by these debates, statistical methods have recently been used to make quantitative statements about the degree of variability and character of transitions. According to their analysis, the most important transition during the long-term trend towards a more arid climate was at ~1.9 Ma, at about the time of the establishment of the modern Walker/Hadley circulation (Ravelo et al., 2004; Trauth et al., 2009; deMenocal, 2012), and not, as suggested earlier by deMenocal (1995, 2004) during the intensification of the Northern Hemisphere Glaciation (INHG). Similarly, the termination of the AHP at ~5 kyr BP was tested for its relative abruptness comparing observed and theoretical probability distributions of paleoclimate time series from multiple locations in and around Africa (Tierney and deMenocal, 2013). According to their analysis, the wet-dry transition occurred within centuries, which agrees with the results of Trauth et al. (2018) using a change point analysis to determine a ~880 yr interval within which this important climate shift occurred.

More sophisticated approaches to classifying variability and transitions were used by Trauth et al. (2019) with recurrence plots together with a recurrence quantification analysis on six short (<17 m) sediment cores collected during the Chew Bahir Drilling Project (CBDP) from the Chew Bahir basin (CHB) in southern Ethiopia, reaching back to ~47 kyr BP. Recurrence plots (RPs) are graphic displays of recurring states in the environmental system (Eckmann et al., 1987; Marwan et al., 2007). Quantitative descriptions (measures of complexity) have been developed to complement visual inspection of recurrence plots (RPs) and for recurrence quantification analysis (RQA) (e.g. Zbilut and Webber 1992; Marwan et al., 2007; Marwan 2008). Trauth et al. (2019) presented and discussed results from such an RQA on the environmental record of the CHB short cores. The different types of variability and transitions in these records were classified to shed light on our understanding of the response of the biosphere to climate change, particularly the response of humans in the area.

One of the most interesting transitions examined with the RP/RQA was once again the termination of the African Humid period (Trauth et al., 2018, 2019). The rapid (~880 yr) change of climate in response to a relatively modest change in orbital forcing appears to be typical of tipping points in complex systems such as the Chew Bahir basin (Lenton et al., 2008; Ditlevsen and Johnsen, 2010). If this is the case then 14 dry events at the end of the AHP, each of them 20–80 yrs long and recurring every 160 ± 40 yrs as documented in the Chew Bahir cores could represent precursors of an imminent tipping point which, if properly interpreted, would allow predictions to be made of future climate change in the Chew Bahir basin (Trauth et al., 2018, 2019). Compared to the low-frequency cyclicity of climate variability before and after the termination of the AHP, this type of cyclicity occurs on time scales equivalent to a few human generations. In other words, it is very likely (albeit speculative) that people were conscious of these changes and adapted their lifestyles to the consequent changes in water and food availability. A deeper analysis of our data is however required to understand whether the wet-dry climate transition in the area

was due to a saddle-node bifurcation in the structural stability of the climate, or whether it was induced by a stochastic fluctuation.

Here we present a RP/RQA-based analysis of two long (~290 m) cores collected in 2014 in the Chew Bahir basin ($4^{\circ}45'40.55''\text{N}$ $36^{\circ}46'0.85''\text{E}$), spanning the time from ~620 kyr to present (Fig. 1). The Chew Bahir basin is situated in a transition zone between the Main Ethiopian Rift and the Omo-Turkana basin, adjacent to the Lower Omo Basin, where some of the oldest known fossils of anatomically modern humans were found (McDougall et al., 2005). According to recent archeological findings, the adjoining highlands in the area may have been a refuge area for groups of *H. sapiens* during times of climatic stress (Ambrose et al., 1998; Brandt and Hildebrand, 2005; Vogelsang et al., 2018; Ossendorf et al., 2019).

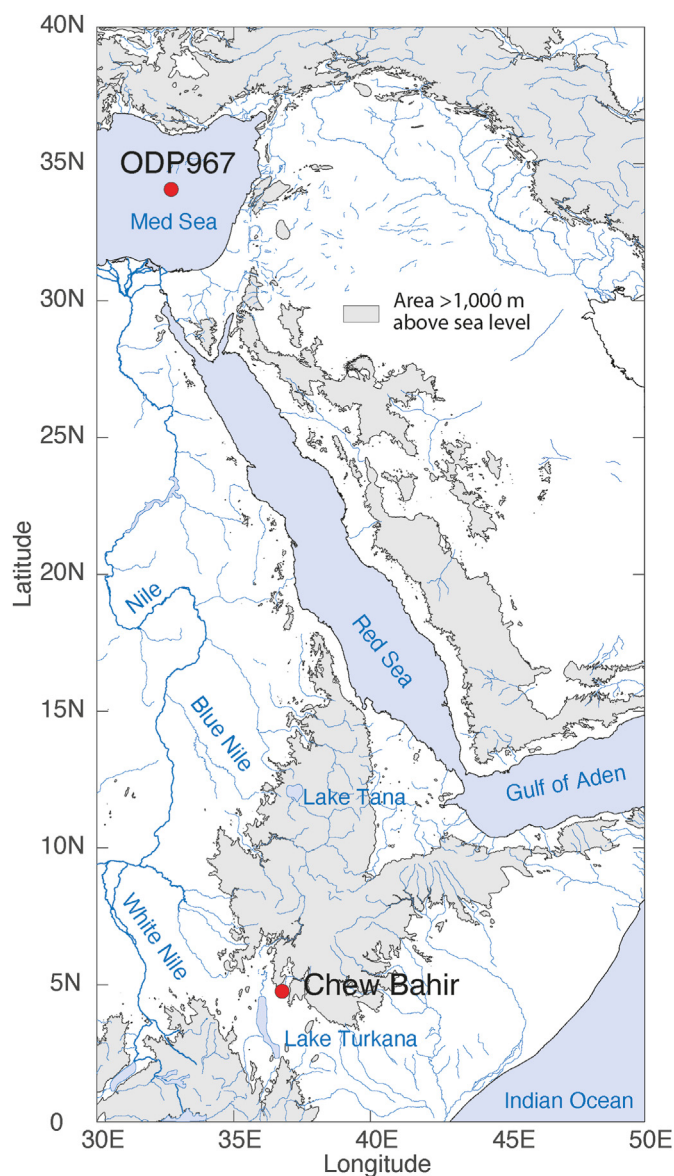


Fig. 1. Map of northeastern Africa and adjacent areas showing the location of the Chew Bahir basin ($4^{\circ}45'40.55''\text{N}$ $36^{\circ}46'0.85''\text{E}$, ~500 m above sea level), the ODP Leg 160 Site 967 in the eastern Mediterranean Sea ($34^{\circ}4'6''\text{N}$ $32^{\circ}43'31''\text{E}$, ~2254 m water depth), and the river Nile with its two tributaries the White and Blue Niles connecting both regions. Coastline and river polygons from the Global Self-consistent, Hierarchical, High-resolution Geography Database (GSHHG) (Wessel and Smith, 1996). Topography from the 1 arc-minute global relief model of the Earth's surface (ETOPO1) (Amante and Eakins, 2009).

We compare the Chew Bahir record of environmental change during the past ~620 kyr with the wetness index for the wider northeastern Saharan/North Africa from Ocean Drilling Program (ODP) Site 967 (Grant et al., 2017) (Fig. 1). The site was drilled during ODP Leg 160 in the eastern Mediterranean (34°N, 34°E, 2252 m water depth), where Saharan and North African dust and Nile riverine input are the primary contributors of sediment. The ODP Site 967 wetness index is a combined run-off and dust signal in a single metric, reflecting the effects of both strengthening/northward migration (increased run-off) and weakening/southward retreat (increased dust) of the northern and northeastern African monsoon (Grant et al., 2017). The catchment of the Nile River with its two tributaries, the White Nile and the Blue Nile, extends from southeastern Africa to parts of the northwestern Ethiopian highlands. In the very wet phases, the Lakes Abaya-Chamo-Chew Bahir-Turkana system with its connecting rivers drained into the Nile catchment (Junginger et al., 2013). Therefore, both the upper Nile catchment and the Chew Bahir catchments are in spatial proximity and are most likely exposed to similar climate fluctuations and their causes. Humid conditions, recorded in both ODP Site 967 and CHB cores, could indicate the regional significance of a wet phase. Similar patterns in the types of variability and transitions could be indicative of the effect of a similar climate dynamic.

As a contribution to the reconstruction of environmental conditions for eastern Africa based on long terrestrial sediment records, our CHB record is firstly used to classify variability down core in order to identify recurring episodes of stable wet or dry, of cyclic or more complex but deterministic variability, and of random variability. Second, we classified types of transitions, including episodes with no change, linear/gradual shifts with different rates of change, as well as different types of rapid transitions such as tipping points. As soon as a classification of variability and transitions is available, one can discuss possible reasons for the similarity, e.g. similar boundary conditions such as global ice volume, local insolation, atmospheric CO₂ levels and ocean sea-surface temperatures. Finally, we hypothesize which types of variability and transitions may have affected the biosphere including hominins.

2. Materials and methods

2.1. The middle Pleistocene–Holocene paleoclimate record of the Chew Bahir basin

The sediment cores described herein were collected in the western part of the Chew Bahir basin in the southern Ethiopian Rift (4.1–6.3°N, 36.5–38.1°E, ~500 above sea level; Fig. 1). Chew Bahir is a tectonic basin, separated from the Lower Omo basin to the west by the Hammar Range, which is the source of most of the sediments at the coring site. This range to the west and the highlands to the north and north-east consist of Late Proterozoic granitic and mafic gneisses, whereas the eastern part of the catchment is dominated by Miocene basaltic lava flows. Oligocene basalt flows with subordinate rhyolites, trachytes, tuffs and ignimbrites cover the Precambrian basement units in the distal north-eastern, northern, and north-western parts of the catchment (Moore and Davidson, 1978; Davidson, 1983). Being a closed basin, Chew Bahir forms a terminal sink for weathering products from its 32,400 km² catchment.

The present-day climate in eastern and northeastern Africa is influenced by a number of major air streams and convergence zones, with their effects superimposed on regional influences associated with topography, large lakes, and the oceans (Nicholson, 2017). Rainfall in the Chew Bahir catchment is associated with the passage of the tropical rain belt, resulting in a strongly bimodal annual cycle. Most of the moisture reaching the Ethiopian highlands in June–August comes from the Mediterranean and Red Sea

(55%), and from the Indian Ocean (31%) (Viste and Sorteberg, 2013). Short-term (annual to decadal) fluctuations in the intensity of precipitation relate to E-W adjustments in the zonal Walker circulation associated with the El Niño–Southern Oscillation (ENSO) and the Indian Ocean Dipole (IOD), possibly as a direct response to sea-surface temperature (SST) variations in the Indian and Atlantic Oceans, which are in turn affected by the ENSO and the IOD (Nicholson, 2017).

The paleoclimate of Chew Bahir was first reconstructed using six short cores, up to ~17 m long and collectively spanning ~47 kyr, which were collected in 2009–2010 (Foerster et al., 2012, 2015; Trauth et al., 2015, 2018, 2019). In the context of the Hominin Sites and Paleolakes Drilling Project (HSPDP) to drill at key fossil hominin and archeological sites (Cohen et al., 2016; Campisano et al., 2017), we collected parallel, duplicate cores: HSPDP-CHB14-2A (4°45′40.32″N 36°46′0.48″E) and 2B (4°45′40.68″N 36°46′1.20″E) in the Chew Bahir basin, 266.38 and 278.58 m long, respectively, in Nov–Dec 2014. A 292.87 m long composite core of the Chew Bahir Drilling Project (CBDP) with more than 90% recovery was created from the duplicate cores.

The composite core was developed by merging the two parallel cores 2A and 2B by core-to-core correlation using MSCL logs, core images, lithological description and XRF data sets. Radiometric age constraints were based on ¹⁴C dating of ostracodes, optically stimulated luminescence (OSL) dating of fine-silt sized quartz grains, and single-crystal total-fusion (SCTF) ⁴⁰Ar/³⁹Ar dating of feldspars from tuffaceous zones within the core. In addition, a volcanic ash layer identified in the core has been correlated on the basis of major and minor element geochemistry to a dated tephra found in the outcrop at Konso, in the southern Main Ethiopian Rift, namely the Silver Tuff (Roberts et al., submitted). The ages generated are stratigraphically consistent, and Bayesian age-depth modeling incorporating ¹⁴C, OSL and ⁴⁰Ar/³⁹Ar ages, and tephrochronological data has been used to build an age model for the Chew Bahir cores (age model RRMarch2021, Roberts et al., 2021). The 1-sigma confidence intervals increase with increasing depth, ranging from <10 kyr in the uppermost 50 m (corresponding to ~100 kyr BP) and 10–35 kyr below 50 m composite depth (~100–620 kyr) (Roberts et al., 2021).

We analyzed the potassium (K) concentrations of the sediment, determined by micro X-ray fluorescence (μXRF) scanning which was previously shown to be a reliable proxy for aridity in the Chew Bahir basin (Foerster et al., 2012; Trauth et al., 2015, 2018). The most likely process linking climate with K count rates is the authigenic illitization of smectites during episodes of higher alkalinity and salinity in the closed-basin lake resulting from a drier climate (Foerster et al., 2018). After processing the μXRF data to remove coring and scanning artifacts, the data were corrected for outliers and jumps, before we applied various types of normalizations and standardizations of the data.

Micro XRF scanning was carried out with a resolution of 5 mm, corresponding to a mean time resolution of ~10 yrs, ranging from ~7 to 50 yrs (Roberts et al., submitted). The K record has been interpolated to an evenly-spaced time axis with a resolution of 100 yrs, corresponding to a ~50 mm (10–70 mm) spatial resolution, using a piecewise cubic Hermite interpolating polynomial (Frisch and Carlson, 1980). This resolution avoids the effects of the scanner's beam width as well as the effects of bioturbation on the signal (e.g. Trauth, 2013), with the exception of large, discrete burrows, which we (as well as other disturbances of the core) have tracked down with the help of core photos and excluded from the interpretation. On the other hand the centennial resolution allows us to investigate the effect of millennium-scale or orbital-scale climatic fluctuations on environmental conditions as well as transitions

over several hundreds or thousands of years.

2.2. Principles of recurrence plots (RP) and recurrence quantification analysis (RQA)

As a first approximation we can describe the Chew Bahir paleolake as a complex system composed of interacting components, such as the water body, the sediment below the bottom of the lake, and the organisms living in the lake and its surroundings (Marwan et al., 2007; Trauth et al., 2019). This multi-dimensional system is characterized by many state variables such as precipitation (with more rain causing higher weathering and erosion of rocks in the catchment, and hence more potassium (K) washed into the lake), evaporation (causing higher K count rates in the sediment through authigenic K fixation in smectites, Foerster et al., 2018) and wind speed (blowing higher quantities of K-rich particles from the catchment into the lake).

One way to unfold the dynamics of the multi-dimensional system from one-dimensional time series is the reconstruction using an embedding procedure (e.g. time delay embedding, Packard et al., 1980). The reason for a complete reconstruction of the system from a single variable is that the information about the system and its state variables is contained in the one-dimensional time series. Time delay embedding of a time series in a three-dimensional ($m = 3$) phase space, for example, means that three successive values with a temporal distance τ (or *tau*) are represented as a point in a three-dimensional coordinate system (the phase space) (Iwanski and Bradley, 1998; Webber and Zbilut, 2005; Marwan et al., 2007). The phase space portrait then displays the dynamics of the system as a trajectory in the phase space, i.e. the phase space trajectory represents the path over which the system's state evolves through time. The reconstruction of the phase space (from embedding) is not exactly the same as the original phase space (the true variables describing the lake), but its topological properties are preserved, provided that the embedding dimension is sufficiently large (Packard et al., 1980; Takens, 1981). The embedding parameters m and τ are selected by an improved false nearest neighbours approach (Hegger and Kantz, 1999) and mutual information (see supplementary information). Before embedding, it is often helpful to filter the time series to improve the signal-to-noise ratio. Here we use a simple nonlinear noise reduction method that is based on phase space averaging (Schreiber, 1993).

A common feature of dynamical systems is the property of recurrence (Webber and Zbilut, 2005). Patterns of recurring states of a system reflect typical system characteristics whose description contributes significantly to understanding the system's dynamics. A recurrence plot (RP), introduced by Eckmann et al. (1987), is a graphical display of such recurring states of the system, calculated from the distance (e.g. Euclidean) between all pairs of observations, within a cutoff limit (Marwan et al., 2007). To complement the visual inspection of recurrence plots, measures of complexity were introduced for their quantitative description to perform the recurrence quantification analysis (RQA) (e.g., Marwan et al., 2007; Marwan, 2008), which have been shown to be successfully applied on even non-stationary paleoclimate data (Donges et al., 2011; Westerhold et al., 2020). Among these, a selection of measures based on the recurrence density, others based on diagonal and vertical lines typically appearing in recurrence plots are very useful for studying the behavior of the Chew Bahir lake system. As an example of measurements based on the recurrence density, the recurrence rate (RR) is the density of black dots in the recurrence plot. This measure simply describes the probability of recurring states of the system in a particular time period.

Diagonal lines in recurrence plots typically occur when a segment of the trajectory runs almost (e.g. within a given tolerance)

in parallel to another segment, representing an earlier episode of the system's history in the phase space, for a certain period of time. Diagonal lines in recurrence plots are therefore diagnostic of cyclic behavior in time series, and in contrast to the time series analysis using Fourier-based methods, this cyclic behavior is not restricted to sinusoidal structures when using recurrence plots. Since cyclic behavior can be used to predict future conditions from the present and past, the ratio of the recurrence points that form diagonal structures (of a minimum length) to all recurrence points is therefore a measure for determinism (DET) of the system.

Although deterministic dynamics does not automatically mean that the dynamics is predictable (e.g., for chaotic systems), a predictable system, however, means that the system is deterministic. Moreover, this definition of determinism is not a strict mathematical one, but more from a heuristic point of view. Vertical lines in recurrence plots typically correspond to periods where the trajectory remains in the same phase space region (Marwan et al., 2007; Marwan, 2010). Vertical lines are therefore diagnostic of episodes when the state of the system does not change or changes very slowly. In other words, the system seems to be trapped in a specific state for some time, which is typical for irregular transitions between different types of dynamics. A more in-depth discussion of the RP/RQA methods, possible problems in the interpretation of the results and suitable solutions to these problems, such as the problem of tangential motion, the importance of the Theiler window and the effect of a trend on results can be found in our earlier work (e.g. Marwan et al., 2007; Trauth et al., 2019).

3. Results

Recurrence plots (RPs), together with a recurrence quantification analysis (RQA), were used to describe different types of environmental variability and transitions in the Chew Bahir (Table 1, Fig. 2 and Suppl. Fig. 1–8). From the available RQA measures we have selected RR and DET because they describe important properties of the dynamic Chew Bahir system but are very descriptive compared to other RQA measures (Marwan et al., 2007; Trauth et al., 2019). We compare the RPs and RQA measures of the Chew Bahir record with those of the wetness index for the wider north-eastern Saharan/North African record from ODP Site 967 (Grant et al., 2017) (Fig. 3).

We have used noise filtered K as a proxy for aridity, as the dominant process linking climate with K count rates is the authigenic illitization of smectites during episodes of higher alkalinity and salinity in the closed-basin lake resulting from a drier climate (Foerster et al., 2018). For the analysis of the ~620 kyr record the K record was embedded in a phase space with a dimension of $m = 6$ and temporal distances of $\tau = 10$ (Suppl. Fig. 7), equivalent to $10 \times 0.1 \text{ kyr} = 1.0 \text{ kyr}$, where 0.1 kyr is the resolution of the time series following a piecewise cubic Hermite interpolating polynomial (Frisch and Carlson, 1980). We use the window size $w = 500$ and the step size $ws = 50$ data points of the moving window to calculate the RQA measures (Fig. 2). The size w of the window corresponds to $500 \times 0.1 \text{ kyr} = 50 \text{ kyr}$ and the step size is $50 \times 0.1 \text{ kyr} = 5 \text{ kyr}$. We use a minimum length of 10 points to compute DET. To compare the RP/RQA based dynamics in the Chew Bahir record of aridity with the wetness index of ODP Site 967, we interpolated the marine record to the same time axis, used the same embedding parameters (Suppl. Fig. 8) to create the RPs and used the same window size to calculate the RQA measures (Fig. 3). Similarities in the texture of the recurrence plots of both proxy records show that the embedding provides comparable results with these values.

The first series of four clusters of recurrence points occurs between 617 and 410 kyr BP in the Chew Bahir record, with the largest cluster between 617 and 462 kyr BP, then three very weak clusters

Table 1

Summary of the RP/RQA results to describe different types of environmental variability and transitions in the Chew Bahir.

	Type 1	Type 2
Occurrence/Time (kyr BP)	617–410 348–272 252–122 107–59 11–0	410–348 272–252 59–11
RP Texture	sparse recurrences longer diagonal lines with larger spacing (5, 10–20 kyr)	dense recurrences block-like structures, short diagonal lines with smaller spacing (1–2 kyr)
Recurrence Quantification	RR low DET low to intermediate (except for the oldest part where DET is also high)	RR intermediate to high DET high

at 456–435, 435–425, and 425–410 kyr BP (Fig. 2). These clusters are structured by a series of partly s-shaped diagonal lines or they represent rather compact blocks with high recurrence rates centered at 610, 505 and 470 kyr, which mark 1–2 kyr long episodes of relative stability. The diagonal lines are 10–15 kyr apart, reflecting a series of wet-dry episodes recurring with approximately half-precession cyclicity, initiated and terminated by relatively abrupt transitions, marked by white vertical lines. As the result of the cyclic recurrence of wet and dry conditions, the DET values are relatively high, whereas RR has moderate, but declining values. Two extremely dry episodes centered at ~455 and ~438 kyr BP are reflected in two clusters of recurrence points and high DET values within the 458–436 kyr BP interval, separated by white vertical lines and slightly lower DET values. Zooming into the interval between 617 and 410 kyr BP with higher (0.015 kyr) resolution the diagonal lines become blurred, are separated by a few thousand years (up to 10 kyr), and the RP is dominated by several small (<10 kyr) blocks that are connected by black horizontal and vertical lines (Suppl. Fig. 1). This suggests that, at time scales of <10 kyr, the system oscillates between shorter stable states, each 1–5 kyr long, with rapid transitions between them. Within the blocks, we observe diagonal lines indicating high-frequency (<1 kyr) cyclicities. The large-scale block and line separation is dominated by 5, 10 and 20 kyr cycles. In the ODP Site 967 wetness index we find a similar type of variability in the time before 435 kyr, although in comparison diagonal structures are much less pronounced or even absent (Fig. 3). The RR values are at similar values to those in the Chew Bahir, except for a significant anticorrelation at ~420 kyr (Fig. 4). The DET values are generally lower but increase after ~500 kyr BP up to similar values as in the Chew Bahir record.

This interval ends with a rapid transition at ~410 kyr BP from dry to wet conditions. This transition is followed by two dense clusters of recurrence points between 410 and 348 kyr BP, indicating episodes of a stable wet climate with extreme RR and DET values (Fig. 2). The two clusters reflect relatively stable humid conditions, with the humidity level in the first cluster being higher than in the second cluster and hence the two clusters are separated by a transition towards a slightly less wet climate at around 390 kyr BP. The second cluster is interrupted by a distinctive dry event at around 376 kyr BP. Interestingly, both clusters show an irregular pattern of diagonal lines, partly slightly curved, suggesting recurrent dry events, but with slightly variable cyclicity. Zooming into the interval between 410 and 348 kyr BP with higher (0.015 kyr) resolution we observe blurred diagonal lines with 1–2 kyr distances in the earlier part before ~390 kyr, with 3–5 kyr in the younger part, indicating a weak cyclicity on millennium time scales even within the otherwise quite stable wet episodes (Suppl. Fig. 2). The interval between 410 and 348 kyr BP is terminated by gradual (~10 kyr) transition towards slightly more humid and more variable conditions after ~348 kyr BP. The ODP Site 967 wetness index

indicates similar wet conditions during this episode, also with relatively low variability (Fig. 3). As a consequence, the RR values are relatively high but decreasing whereas the DET values are also at high level but relatively low compared to before and after the event.

The next cluster of recurrence points between 348 and 272 kyr BP is marked by a series of blocks with weak internal structure and separated by white vertical lines (Fig. 2). This structure reflects a series of relatively stable wet conditions, interrupted by several thousand-year long dry episodes, some of which are bounded by relatively rapid transitions from wet to dry and back. The occasional appearance of diagonal lines, though rarely parallel to the main diagonal, indicates weak cyclic behavior. Within this interval the RR values are constantly low, whereas the DET values start at high values and decline until about 320 kyr BP before they remain at low values. Zooming into the interval between 348 and 272 kyr BP with higher (0.015 kyr) resolution confirms the observation of small blocks connected with black horizontal and vertical lines in the RP, as a result of a rapid change between relatively stable dry and wet conditions, with the exception of the block between 330 and 327 kyr BP. This block is merely the result of a gap that was closed by interpolation (Suppl. Fig. 3). The blocks themselves have little internal structure, with the exception of very weak diagonal lines with a spacing of 1–2 kyr. The interval between 348 and 272 kyr BP is terminated by a very rapid transition from wet to dry conditions at ~272 kyr. The ODP Site 967 wetness index shows a similar variability type during this episode, but with higher DET values remaining at high levels compared to those of the Chew Bahir (Fig. 3).

Between 272 and 252 kyr BP, we observe another dense cluster of recurrence points (Fig. 2). The internal structure of this block is reminiscent of similar structures of the clusters at ~400 and ~360 kyr BP, whereas the system state based on the difference in the DET values does not support this conclusion. The interval again shows very weak diagonal lines. As a result of this cyclicity, the RR and DET values are at moderate levels, with DET at a local maximum. This pattern suggests that the climate was relatively stable, but fluctuations between humid and dry occur in cycles. These changes occur more and more frequently over time, until the climate finally quickly changes to generally humid conditions at around 228 kyr BP. Zooming into the interval between 272 and 252 kyr BP with higher (0.015 kyr) resolution reveals that the curved diagonal lines are rather a sequence of short, laterally offset diagonal pieces. In the younger section of the block, the diagonal lines disappear (Suppl. Fig. 4). Considering the course of the time series it can be seen that the diagonals reflect increasingly shorter wet phases, and until after about 236 kyr quite stable, relatively dry conditions prevail in the Chew Bahir. The ODP Site 967 wetness index shows similar climate fluctuations during this episode, but these are too unclear to be described with a different type of variability (Fig. 3).

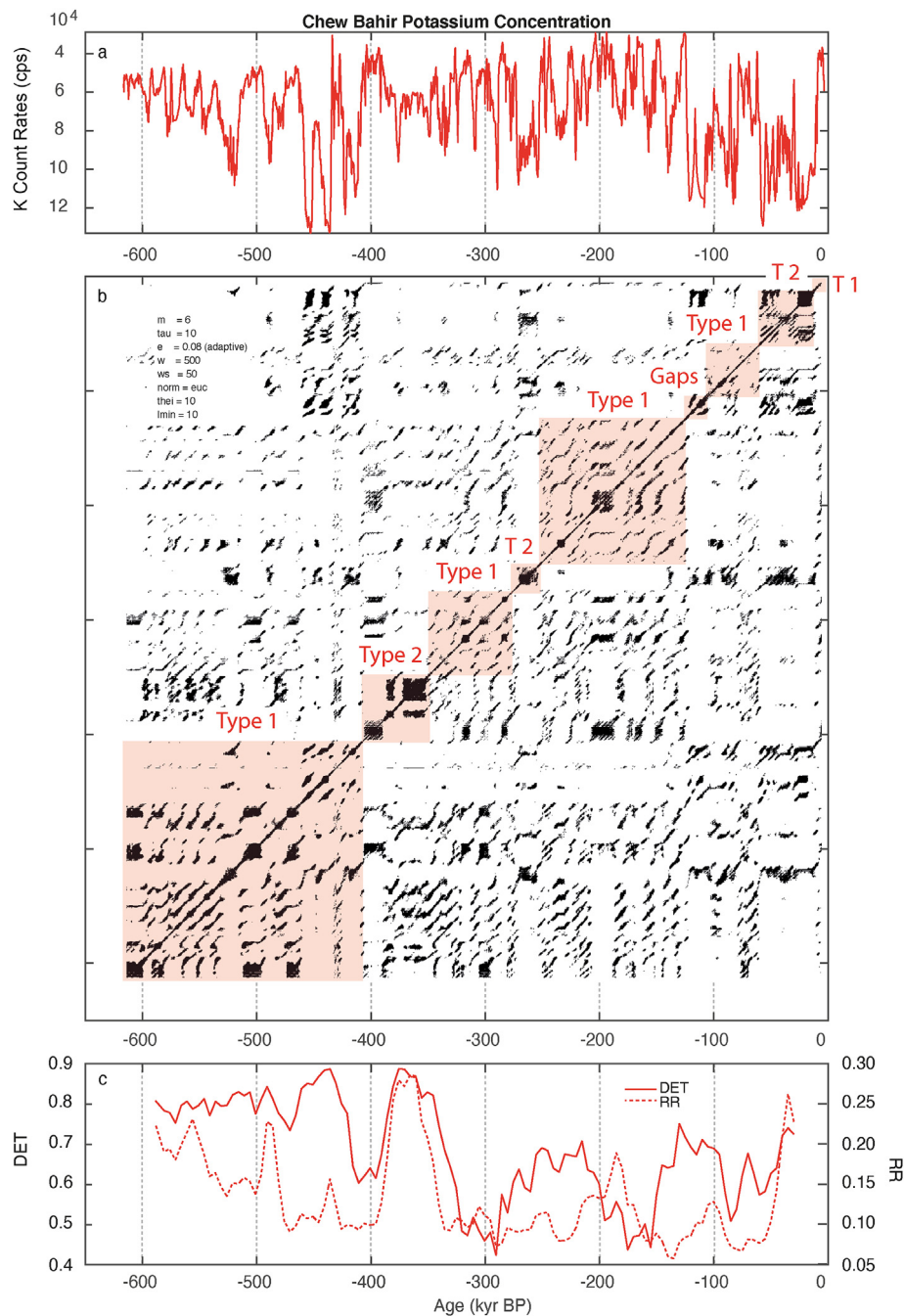


Fig. 2. Recurrence plot (RP) and recurrence quantification analysis (RQA) measures of the potassium (K) count rates of the sediment in Chew Bahir, southern Ethiopia: the time series according to age model (3) (upper panel), the recurrence plot (middle panel) and the RQA measures of moving windows (lower panel). Embedding parameters m = embedding dimension, τ = time delay, e = threshold, w = window size, ws = window moving steps, $norm$ = vector norm, $thei$ = size of Theiler window, $lmin$ = minimum line length, RQA measures RR = recurrence rate and DET = determinism. See the methods section for a detailed description of the embedding parameters and RQA measures.

The RR values are low, similar to those in the Chew Bahir, whereas the DET values rise sharply, probably because of subsequent long-wave cyclicities, in contrast to the Chew Bahir.

The episode between 252 and 122 kyr BP mirrors the earlier ones between 617 and 410 kyr BP and between 348 and 272 kyr BP, whereby in the second interval also the state of the environmental system also recurs. The episode is unfortunately followed by two gaps due to core loss between ~122 and 107 kyr BP, which are filled by the interpolation with curves, so we get a high RR at this point that we cannot interpret (Fig. 2). Zooming into the interval between 252 and 122 kyr BP with higher (0.015 kyr) resolution reveals many

small blocks surrounded by s-shaped curved structures rather than continuous diagonal lines which mark short (<5 kyr) wet phases which begin and end gradually (Suppl. Fig. 5). Besides that, we observe longer (5–10 kyr) wet episodes with rapid onset and termination, internally structured by converging diagonals, structurally similar to the ones in the interval between 272 and 252 kyr BP, but with a different system state based on the RR and DET values. This interval is terminated by ~5 kyr long gaps after 122 kyr BP. During this episode, the ODP Site 967 wetness index shows a type of variability that is more similar to the episode of 435 and 370 kyr BP, rather than the one after 370 kyr BP (Fig. 3). The course of

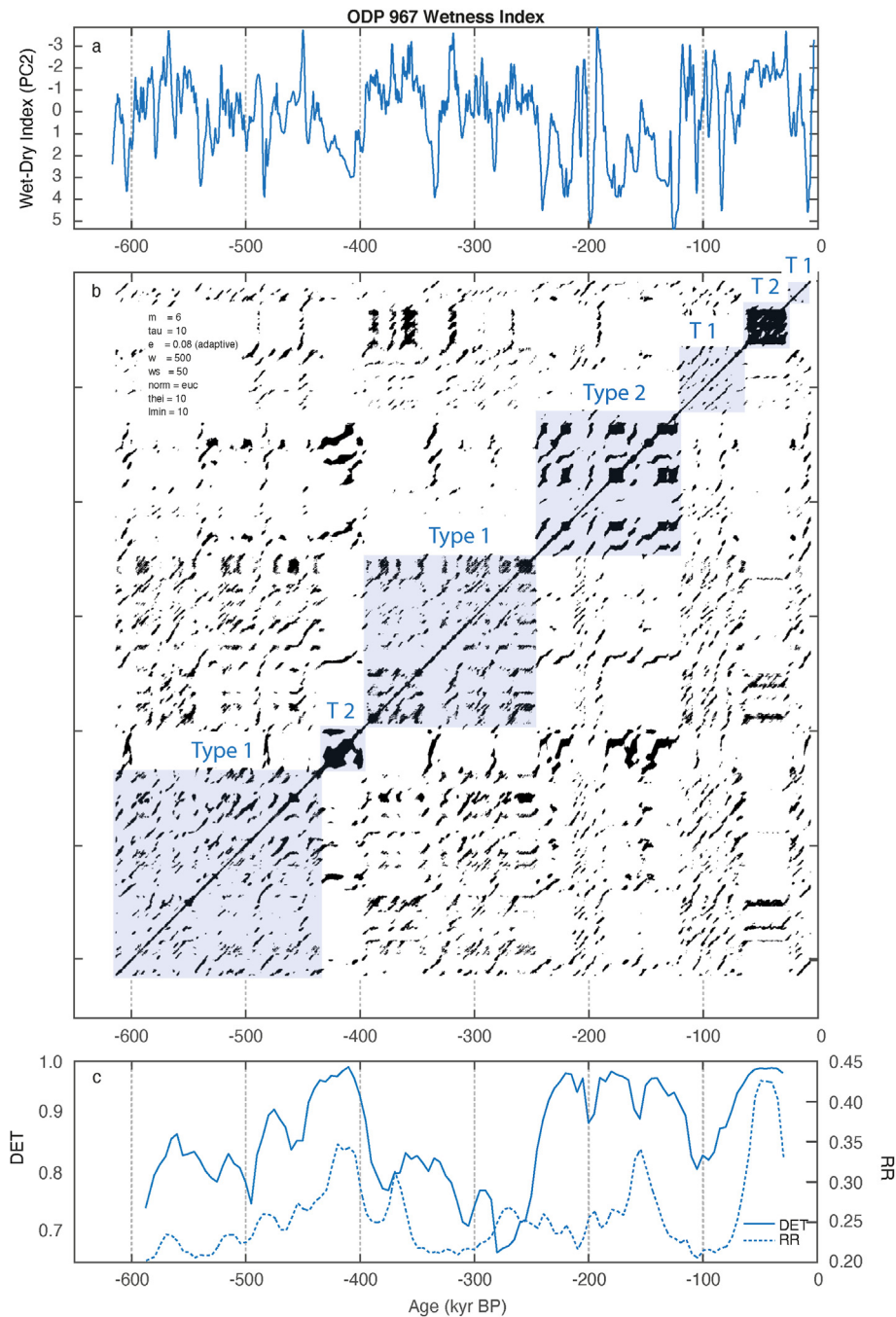


Fig. 3. Recurrence plot (RP) and recurrence quantification analysis (RQA) measures of the ODP Site 967 wetness index according to Grant et al. (2017) from the eastern Mediterranean: the time series (upper panel), the recurrence plot (middle panel) and the RQA measures of moving windows (lower panel). See previous figure for the meaning of the abbreviations. For abbreviations, see caption of Fig. 2. See the methods section for a detailed description of the embedding parameters and RQA measures.

the RR values is similar to the one of Chew Bahir in the first half of the interval, but seems to be anticorrelated in the second half. The DET values show a very similar pattern to those of the Chew Bahir, although at higher levels. The increasing DET values at the beginning of the interval are about 20 kyr later for ODP Site 967, then they vary in a very similar way even including a minimum at about 160 kyr, and then decline at the end of this interval (Fig. 4).

Between 107 and 59 kyr BP, we find a very complex phase with fast changes between stable humid, very variable humid and very dry conditions, each separated by fast transitions (Fig. 2 and Suppl. Fig. 6). After a very dramatic transition we observe very

regular climate fluctuations between ~59 kyr BP and about 11 kyr BP, when it became relatively stable dry. This interval is again characterized by a cluster of dense recurrence points, slightly converging diagonal lines which indicate increasing recurrence rates (i.e. shorter wet-dry cycles), before we see a black block of recurrence points as the result of very stable dry conditions. The last ~11 kyr are characterized by very wet conditions, interrupted with a short, about ~1 kyr long dry intervals and terminated by a transition towards a dry climate. The distinct cyclic alternation of wet and dry conditions, each of which are ~5 kyr long, results in high RR and DET values. The last ~47 kyr BP are preserved at higher

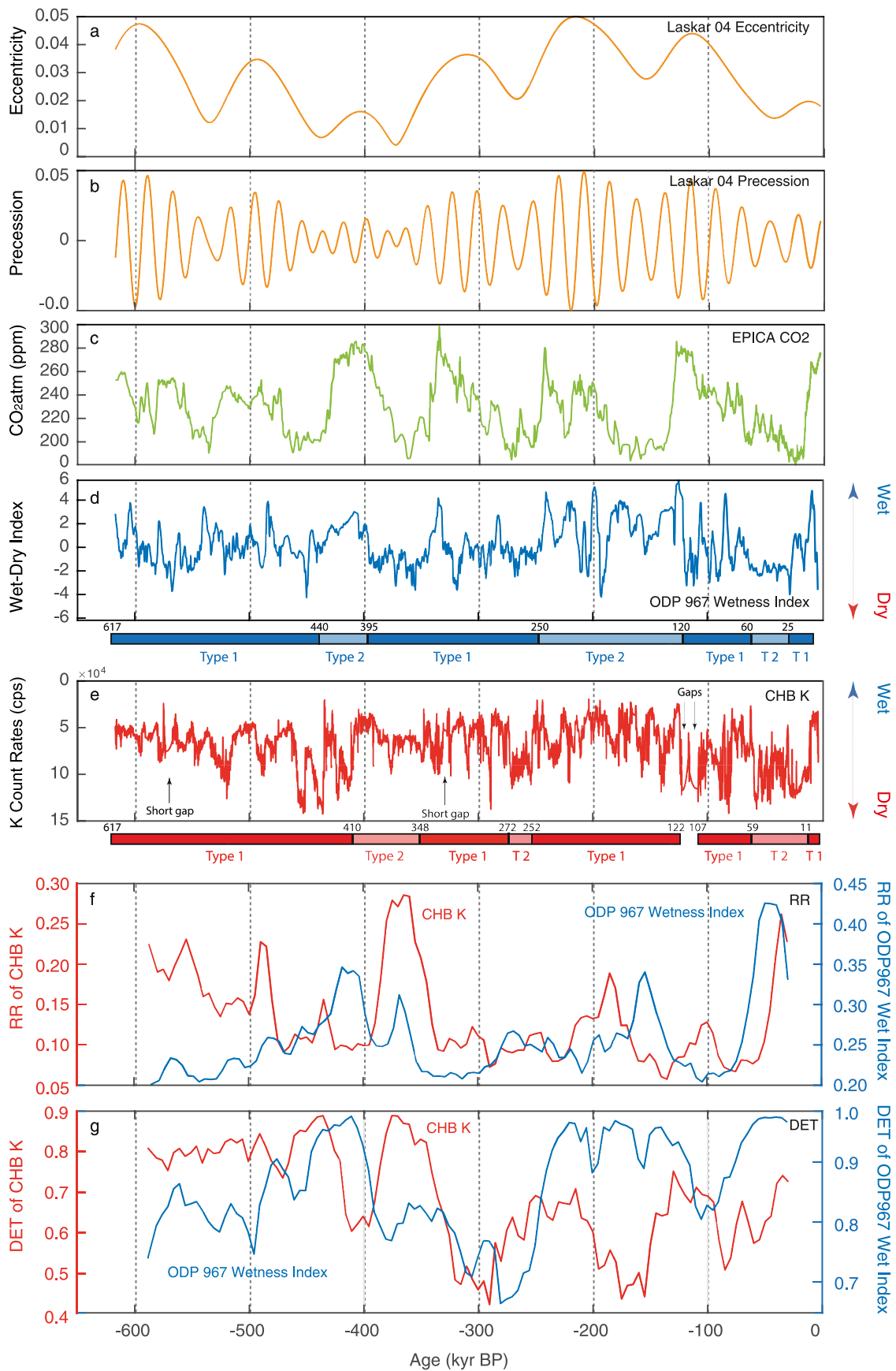


Fig. 4. Comparison of the complex dynamics of variations in aridity in southern Ethiopia with strengthening/northward migration and weakening/southward retreat of the North African monsoon. (a+b) Earth's eccentricity and precession cycle (Laskar et al., 2004); (c) Antarctica EPICA Dome C atmospheric CO₂ according to Bereiter et al. (2015); (d) ODP Site

resolution in the short cores from the same basin, also examined with the method of RP/RQA (Trauth et al., 2019). Here we found very similar patterns as on the long time scale, with alternating appearances of blocky structures and diagonal lines, with different transitions between episodes. The ODP Site 967 wetness index here shows a similar variability with long-periodic, high amplitude fluctuations between wet and dry between ~120 and 60 kyr BP, followed by an episode without such variations (Fig. 3). The time interval between 60 and 25 kyr BP is relatively stable, as compared with the high-frequency variability observed in the Chew Bahir, before we observe two long wet cycles, out of which the second one is also seen in the Chew Bahir record.

4. Discussion

We applied a detailed analysis of the RPs together with a RQA to distinguish between different types of climate variability, and transitions in the Chew Bahir basin (Trauth et al., 2018) (Fig. 4). Here, climate is inferred from our key proxy, the potassium concentration of the sediment representing the relative aridity in the Chew Bahir Basin (Foerster et al., 2018). Our statistical analyses herein are a contribution to an accurate picture of environmental change in eastern Africa during the last ~620 kyr and thereby provide a quantitative, high resolution climatic component useful for investigating human-climate interactions. The fossil and archeological record of eastern Africa is still too limited to draw definitive conclusions with respect to current hypotheses on the relationship between climate and evolutionary patterns in humans and other animals. However, our results do allow for some initial comparisons and hypotheses (e.g. Stringer and Galway-Witham, 2017; Scerri et al., 2018; Galway-Witham et al., 2019).

Our analysis clearly shows a number of different types of variability in the K record that overlay a long-term trend towards greater aridity and variability (Figs. 2 and 4). These types of variability are separated by transitions, which are of varying types of durations and structures. Many of these types, both variability and transitions, occur multiple times during the last ~620 kyr, so it is interesting to investigate them more closely to see if they are characteristic of the Chew Bahir Basin or possibly occur even beyond the region. In addition, it is important to examine whether these types are linked to certain regional or global boundary conditions (e.g. global ice volume, atmospheric CO₂ levels, ocean sea-surface temperatures) (Fig. 4).

We observe two basic types of variability that do not mix, but each form a series of variants. The first type of variability, occurring at 617–410 kyr BP, 348–272 kyr BP, 252–122 kyr BP, and (after a period with no data) 107–59 kyr BP, are slow variations with cycles of ~20 kyr and subharmonics of this cycle, as indicated by the occurrence of diagonal lines with 20 kyr, 10 kyr, and 5 kyr spacing (Figs. 2 and 3). In addition to these cyclical wet-dry fluctuations in the area, extreme events often occur, i.e. short wet or dry episodes, lasting for several centuries or even millennia, and rapid transitions between wet and dry episodes. This type of variability probably reflects the influence of precessional forcing in the lower latitudes at times of increased eccentricity, with a tendency towards extreme events. This also shows in comparatively low RR and DET values, suggesting a lower determinism of climate variations for this type of variability. This type of variability correlates with maximum values of the long (400 kyr) eccentricity cycle, and hence maximum variability in the precession frequency band. There does not seem

to be a systematic correlation with atmospheric CO₂ concentration within this type of variability.

The second type of variability, occurring at 410–348 kyr BP, 272–252 kyr BP, and 59–11 kyr BP, is characterized by relatively low variation on orbital time scales. Instead, we observe significant century-millennium-scale variations with increasing frequency in the course of an episode with Type 2 variability, as block-like pattern with thin diagonal lines of short spacing suggest (Figs. 2 and 3). The very prominent cycles in the frequency band lead to very high DET and partly high RR values, which indicate a higher deterministic regime of climate change, much higher than at times of Type 1. Within this type of variability there are extremely fast transitions between dry and wet within a few decades or years, in contrast to those within Type 1 with transitions that last several hundreds of years. Type 2 variability seems to be linked with minimum values of the long (400 kyr) eccentricity cycle, and again there does not seem to be a link with atmospheric CO₂ levels. The first episode with Type 2 variability occurs in an interval with maximum eccentricity in the 100 kyr frequency band when the atmospheric CO₂ was quite high. The other two episodes occur during minimal eccentricity in this frequency band, with low CO₂ levels at the same time.

The ODP Site 967 wetness index shows a very similar type of variability, with RR values that highly resemble the variations in the Chew Bahir record, except for the prominent anticorrelation at ~420 and ~150 kyr BP (Fig. 4). The DET values fluctuating in a smaller range compared to those of the Chew Bahir, but the temporal variations of DET show obvious similarities at both sites, in particular during the last ~350 kyr. Since the age models of both sites have large uncertainties, it is not possible at this point to judge conclusively whether time shifts in the DET curves are the result of poor age control or actual differences in climate dynamics recorded in the two locations. Comparing the temporal occurrence of the different types of variability in both localities, the ODP Site 967 wetness index shows a Type 2 variability approximately during the first and third episode of Type 2 variability in the Chew Bahir record, but not during the second episode of Type 2 variability in the Chew Bahir. Instead we find a Type 2 variability between ~245 and 120 kyr BP in the ODP Site 967 wetness index, all with high DET and RR values. The different types of variability, very obvious in the RPs, but differing slightly in the RQA measures, could also indicate actual differences in dynamics, but also the influence of the spline interpolation on the temporal autocorrelation.

Overall, the K curve shows a clear trend towards a drier and more variable climate, most prominently during the last 200 kyr, which is also reflected in the reducing DET and RR values (Fig. 4). The three episodes with Type 2 variability are about the same length (45–60 kyr) but have (according to the long-term trend) decreasing average humidity levels. The first episode is characterized by a very humid climate, while the two later episodes were rather dry. In particular, the DET values show several stepwise declines over the entire time series, which are not compensated by corresponding increases. The most striking declines are centered at approximately 480 kyr BP, 420 kyr BP, 330 kyr BP, 200 kyr BP, 180 kyr BP and 90 kyr BP. The most dramatic increases in DET are centered at approximately 460 kyr BP, 385 kyr BP, 285 kyr BP, 255 kyr BP, 150 kyr BP and 75 kyr BP. The variability also increased, especially if a few larger fluctuations between 460 and 410 kyr, at ~335 kyr BP and at ~245 kyr BP are disregarded. In addition, the frequency of rapid transitions from dry to wet and back increases

967 wetness index according to Grant et al. (2017); (e) Chew Bahir aridity derived from the potassium (K) concentrations of the sediment in Chew Bahir using age model RRMarch2021 (Roberts et al., submitted), note the reverse y-axis; (f + g) comparison of RQA measures determinism (DET) and recurrence rate (RR) of the recurrence plots (RP) of the Chew Bahir aridity record (in red) and ODP Site 967 wetness index (in blue). DET is a measure of the determinism of the system and RR describes the probability of recurring states of the system in a particular time period.

over time. The ODP Site 967 record shows similar trends on long time scales, whereas there are large differences on shorter time scales, especially in the degree of variability.

The different types of variability and the transitions between these types have important implications for our understanding of the availability of water. Different modes of variability would have transformed eastern Africa's environment considerably, including its vegetation and fauna, and would have shaped the habitat of hominins, including archaic and modern *H. sapiens*, in that part of the continent. The central question, however, is to what extent the different types of fluctuations observed in the environmental record of the Chew Bahir have actually had an impact on living conditions of hominins. Overall, long-term changes (>1 kyrs) would have formed the living environment of hominins on a time-scale that responds to human evolution and corresponds to a time window that is long enough to facilitate large-scale dispersal. The short-term fluctuations (<1 kyrs) may have had dramatic consequences for populations including differential mortality/fertility of *H. sapiens* down to the level of individuals, and thus short-term changes in behavior, including evasive movements to more favorable habitats (e.g. Foerster et al., 2015).

To assess the impact of climate variability on people, it is worth using a well-studied younger analogue of hydroclimatic transformation in eastern Africa. The most recent example of a wet-to-dry transition within Type 1 was the time-progressive termination of the African Humid Period (AHP, 15–5 kyr BP), which lasted several hundred years in most areas (Shanahan et al., 2015; Trauth et al., 2018). At this time, a previously green, then yellow Sahara was largely depopulated, but this happened quite slowly and due to the time-transgressive termination rather in the form of people slowly following favorable living conditions (Kuper and Kröpelin, 2006; Kröpelin et al., 2008a, b; Shanahan et al., 2015). During this gradual transition, climate deterioration could have fostered an important socio-economic transition, including the transition from hunter-gatherer to pastoralism (Garcin et al., 2012; Foerster et al., 2015).

In contrast, the most recent example of a wet-to-dry transition within Type 2 is the onset of pronounced arid conditions during the Younger Dryas chronozone (YD, ~12.8–11.6 kyr BP) that occurred within ~45 yr at Chew Bahir (Trauth et al., 2018). Most importantly, millennial-scale transitions such as the YD happened everywhere at the same time, unlike the orbital-controlled slow changes (Shanahan et al., 2015; Trauth et al., 2018). It is implausible that such relatively rapid transitions triggered a fundamental societal transformation, similar to the one during the termination of the AHP. Instead, climate shifts of this rapidity would allow response patterns that are implementable within (less than) a life-time span, such as short-term migration towards proximal more favorable living conditions. Examples of this are movements from hot dry low-lands into still vegetation-rich high altitudes, or even the complete disappearance of entire local human populations due to scarcity of resources (Foerster et al., 2015, 2018). The possible alternative response to environmental extremes and too fast transformation is extinction/extirpation, because living conditions deteriorated so quickly that neither physical nor cultural adaptation was possible. However, short-term and short-distance mobility depends (a) on a number of socio-cultural conditions (= how flexible, how adaptable are groups, how are they organized?) and (b) mode of climatic change (= pulsed, rapid, parallel with other areas).

5. Conclusions

We find two types of variability in the Chew Bahir record, (1) Type 1 probably reflecting the influence of a precessional forcing in

the lower latitudes at times of increased eccentricity, with the tendency towards extreme events, and (2) Type 2 with significant century-millennium-scale variations with increasing frequency. Within Type 2 of variability there are extremely fast transitions between dry and wet within a few decades or years that would have exerted a high level of climatic stress on the biosphere including humans, in contrast to those within Type 1 with transitions within several hundreds of years. As the body of archeological evidence, including fossils and diagnostic tools, continues to increase in the future, it will be exciting to compare potential response patterns to our proposed Type 2 phases of high climatic stress and see whether changes in settlement activities, cultural innovation, or even the emergence or disappearance of populations/occupancy can be correlated with the climatic dimension of the complex framework in human-climate interactions.

Data availability

The Chew Bahir potassium record and all MATLAB scripts will be made available at <http://mres.uni-potsdam.de>.

Author statement

Martin H. Trauth: Conceptualization, Methodology, Software, Formal analysis, Writing—Original Draft, Funding acquisition. Asfawossen Asrat: Conceptualization, Writing – review & editing, Funding acquisition. Andrew S. Cohen: Conceptualization, Writing – review & editing, Funding acquisition. Walter Duesing: Validation, Writing – review & editing. Verena Foerster: Investigation, Writing – review & editing. Stefanie Kaboth-Bahr: Validation, Investigation, Writing – review & editing. K. Hauke Kraemer: Methodology, Software, Formal analysis, Visualization, Writing—Original Draft. Henry F. Lamb: Conceptualization, Writing – review & editing, Funding acquisition. Norbert Marwan: Methodology, Software, Formal analysis, Writing—Original Draft. Mark A. Maslin: Investigation, Writing – review & editing. Frank Schäbitz: Conceptualization, Writing – review & editing, Funding acquisition.

Declaration of competing interest

The authors declare that they have no known competing financial interests or personal relationships that could have appeared to influence the work reported in this paper.

Acknowledgements

Support for HSPDP has been provided by the National Science Foundation (NSF) grants and the International Continental Drilling Program (ICDP). Support for CBDP has been provided by Germany Research Foundation (DFG) through the Priority Program SPP 1006 ICDP (SCHA 472/13 and/18, TR 419/8,10 and/16) and the CRC 806 Research Project “Our way to Europe” Project Number 57444011. Support has also been received from the UK Natural Environment Research Council (NERC, NE/K014560/1, IP/1623/0516). We also thank the Ethiopian permitting authorities to issue permits for drilling in the Chew Bahir basin. We also thank the Hammar people for the local assistance during drilling operations. We thank DOS-ECC Exploration Services for drilling supervision and Ethio Der pvt. Ltd. Co. For providing logistical support during drilling. Initial core processing and sampling were conducted at the US National Lacustrine Core Facility (LacCore) at the University of Minnesota. We thank Christopher Bronk Ramsey, Melissa Chapot, Alan Deino, Christine S. Lane, Helen M. Roberts and Céline Vidal for discussions

on the geochronology and age modeling. S.K.B. has received further financial support from the University of Potsdam Open Topic Postdoc Program. This is publication 29 of the Hominin Sites and Paleolakes Drilling Project.

Appendix A. Supplementary data

Supplementary data to this article can be found online at <https://doi.org/10.1016/j.quascirev.2020.106777>.

References

- Amante, C., Eakins, B.W., 2009. ETOPO1 1 Arc-Minute Global Relief Model: Procedures, Data Sources and Analysis, vol. 24. NOAA Technical Memorandum NESDIS NGDC. <https://doi.org/10.7289/V5C8276M>.
- Ambrose, S.H., 1998. Late Pleistocene human population bottlenecks, volcanic winter, and the differentiation of modern humans. *J. Hum. Evol.* 35, 115–118. <https://doi.org/10.1006/jhev.1998.0219>.
- Bereiter, B., Eggelston, S., Schmitt, J., Nehrbass-Ahles, C., Stocker, T.F., Fischer, H., Kipfstuhl, S., Chappellaz, J., 2015. Revision of the EPICA Dome C CO₂ record from 800 to 600 kyr before present. *Geophys. Res. Lett.* 42, 542–549. <https://doi.org/10.1002/2014GL061957>.
- Bonnefille, R., 2010. Cenozoic vegetation, climate changes and hominid evolution in tropical Africa. *Global Planet. Change* 72, 390–411. <https://doi.org/10.1016/j.gloplacha.2010.01.015>.
- Brandt, S.A., Hildebrand, E.A., 2005. Southwest Ethiopia as an upper pleistocene refugium. In: Paper Presented at the Workshop on the Middle Stone Age of Eastern Africa. Nairobi, Kenya and Addis Ababa, Ethiopia, July 2005.
- Brovkin, V., Claussen, M., 2008. Comment on "Climate-Driven ecosystem succession in the Sahara: the past 6000 yr. *Science* 322. <https://doi.org/10.1126/science.1163381>, 1326b–c.
- Campisano, C.J., Cohen, A.S., Arrowsmith, J.R., Asrat, A., Behrensmeyer, A.K., Brown, E.T., Deino, A.L., Deocampo, D.M., Feibel, C.S., Kingston, J.D., Lamb, H.F., Lowenstein, T.K., Noren, A., Olago, D.O., Owen, R.B., Pelletier, J.D., Potts, R., Reed, K.E., Renaud, R.W., Russell, J.M., Russell, J.L., Schabitz, F., Stone, J.R., Trauth, M.H., Wynn, J.G., 2017. The hominin sites and paleolakes drilling project: high-resolution paleoclimate records from the east african Rift system and their implications for understanding the environmental context of hominin evolution. *PaleoAnthropology* 2017, 1–43. <https://doi.org/10.4207/PA.2017.ART104>.
- Cane, M.A., Molnar, P., 2001. Closing of the Indonesian seaway as a precursor to east African aridification around 3–4 million years ago. *Nature* 411, 157–162. <https://doi.org/10.1038/35075500>.
- Cohen, A., Campisano, C., Arrowsmith, R., Asrat, A., Behrensmeyer, A.K., Deino, A., Feibel, C., Hill, A., Johnson, R., Kingston, J., Lamb, H., Lowenstein, T., Noren, A., Olago, D., Owen, R.B., Potts, R., Reed, K., Renaud, R., Schabitz, F., Tiercelin, J.-J., Trauth, M.H., Wynn, J., Ivory, S., Brady, K., O'Grady, R., Rodysill, J., Githiri, J., Russell, J., Foerster, V., Dommain, R., Rucina, S., Deocampo, D., Russell, J., Billingsley, A., Beck, C., Dorenbek, G., Dullo, L., Feary, D., Garello, D., Gromig, R., Johnson, T., Junginger, A., Karanja, M., Kimburi, E., Mbutia, A., McCartney, T., Muiruri, E., Muiruri, V., Nambiro, E., Negash, E.W., Njagi, D., Wilson, J.N., Rabideaux, N., Raub, T., Sier, M.J., Smith, P., Urban, J., Warren, M., Yadeta, M., Yost, C., Zinaye, B., 2016. The hominin sites and paleolakes drilling project: inferring the environmental context of human evolution from eastern african Rift lake deposits. *Sci. Drill.* 21, 1–16. <https://doi.org/10.5194/sd-21-1-2016>.
- Davidson, A., 1983. The Omo river project: reconnaissance geology and geochemistry of parts of ilubabor, kefa, gemu gofa and sidamo. *Ethiop. Inst. Geol. Surv. Bull.* 2, 1–89.
- deMenocal, P., 1995. Plio-pleistocene african climate. *Science* 270, 53–59. <https://doi.org/10.1126/science.270.5233.53>.
- deMenocal, P., Ortiz, J., Guilderson, T., Adkins, J., Sarinthein, M., Baker, L., Yarusinsky, M., 2000. Abrupt onset and termination of the African Humid Period: rapid climate responses to gradual insolation forcing. *Quat. Sci. Rev.* 19, 347–361. [https://doi.org/10.1016/S0277-3791\(99\)00081-5](https://doi.org/10.1016/S0277-3791(99)00081-5).
- deMenocal, P.B., 2004. African climate change and faunal evolution during the Pliocene-Pleistocene. *Earth Planet. Sci. Lett.* 220, 3–24. [https://doi.org/10.1016/S0012-821X\(04\)00003-2](https://doi.org/10.1016/S0012-821X(04)00003-2).
- deMenocal, P.B., 2012. The Ocean's Role in the Early Pleistocene Aridification of East Africa. American Association for the Advancement of Science Annual Meeting, Vancouver, Canada.
- Ditlevsen, P.D., Johnsen, S.J., 2010. Tipping points: early warning and wishful thinking. *Geophys. Res. Lett.* 37, L19703. <https://doi.org/10.1029/2010GL044486>.
- Donges, J.F., Donner, R.V., Trauth, M.H., Marwan, N., Schellnhuber, H.J., Kurths, J., 2011. Nonlinear detection of paleoclimate-variability transitions possibly related to human evolution. *Proc. Natl. Acad. Sci. U. S. A* 108 (51). <https://doi.org/10.1073/pnas.1117052108>.
- Eckmann, J.P., Kamphorst, S.O., Ruelle, D., 1987. Recurrence plots of dynamical systems. *Europhys. Lett.* 5, 973–977. <https://doi.org/10.1209/0295-5075/4/9/004>.
- Foerster, V., Deocampo, D.M., Asrat, A., Günter, C., Junginger, A., Kraemer, H., Stronck, N.A., Trauth, M.H., 2018. Towards an understanding of climate proxy formation in the Chew Bahir basin, southern Ethiopian Rift. *Palaeogeogr. Palaeoclimatol. Palaeoecol.* 501, 111–123. <https://doi.org/10.1016/j.palaeo.2018.04.009>.
- Foerster, V., Junginger, A., Langkamp, O., Gebru, T., Asrat, A., Umer, M., Lamb, H., Wennrich, V., Rethemeyer, J., Nowaczyk, N., Trauth, M.H., Schabitz, F., 2012. Climatic change recorded in the sediments of the Chew Bahir basin, southern Ethiopia, during the last 45,000 yr. *Quat. Int.* 274, 25–37. <https://doi.org/10.1016/j.quaint.2012.06.028>.
- Foerster, V., Vogelsang, R., Junginger, A., Asrat, A., Lamb, H.F., Schabitz, F., Trauth, M.H., 2015. Environmental change and human occupation of southern Ethiopia and northern Kenya during the last 20,000 yr. *Quat. Sci. Rev.* 129, 333–340. <https://doi.org/10.1016/j.quascirev.2015.10.026>.
- Fritsch, F.N., Carlson, R.E., 1980. Monotone piecewise cubic interpolation. *SIAM J. Numer. Anal.* 17, 238–246. <https://doi.org/10.1137/0717021>.
- Galway-Witham, J., Cole, J., Stringer, C., 2019. Aspects of human physical and behavioural evolution during the last 1 million years. *J. Quat. Sci.* 34, 355–378. <https://doi.org/10.1002/jqs.3137>.
- Garcin, Y., Melnick, D., Strecker, M.R., Olago, D., Tiercelin, J.J., 2012. East African mid-Holocene wet–dry transition recorded in palaeo-shorelines of Lake Turkana, northern Kenya Rift. *Earth Planet. Sci. Lett.* 331–332, 322–334. <https://doi.org/10.1016/j.epsl.2012.03.016>.
- Grant, K.M., Rohling, E.J., Westerhold, H., Zabel, M., Heslop, D., Konijnendijk, T., Lourens, L., 2017. A 3 million year index for North African humidity/aridity and the implication of potential pan-African humid periods. *Quat. Sci. Rev.* 171, 100–118. <https://doi.org/10.1016/j.quascirev.2017.07.005>.
- Hegger, R., Kantz, H., 1999. Improved false nearest neighbor method to detect determinism in time series data. *Phys. Rev. E* 60, 4970. <https://doi.org/10.1103/PhysRevE.60.4970>.
- Iwanski, J., Bradley, E., 1998. Recurrence plot analysis: to embed or not to embed? *Chaos* 8, 861–871. <https://doi.org/10.1063/1.166372>.
- Junginger, A., Trauth, M.H., 2013. Hydrological constraints of paleo-lake suguta in the northern Kenya Rift during the african humid period (15–5 ka BP). *Global Planet. Change* 111, 174–188. <https://doi.org/10.1016/j.gloplacha.2013.09.005>.
- Kröpelin, S., Verschuren, D., Lézine, A.M., 2008b. Response to comment on "Climate-Driven ecosystem succession in the Sahara: the past 6000 years. *Science* 322, 1326. <https://doi.org/10.1126/science.1163483>.
- Kröpelin, S., Verschuren, D., Lézine, A.-M., Eggermont, H., Cocquyt, C., Francus, P., Cazet, J.-P., Fagot, M., Rumes, B., Russell, J.M., Darius, F., Conley, D.J., Schuster, M., von Suchodoletz, H., Engstrom, D.R., 2008a. Climate-driven ecosystem succession in the Sahara: the past 6000 yr. *Science* 320, 765–768. <https://doi.org/10.1126/science.1154913>.
- Kuper, R., Kröpelin, S., 2006. Climate-controlled holocene occupation in the Sahara: motor of Africa's evolution. *Science* 313. <https://doi.org/10.1126/science.1130989>, 803–307.
- Laskar, J., Gastineau, M., Joutel, F., Robutel, P., Levrard, B., Correia, A., 2004. A long term numerical solution for the insolation quantities of Earth. *Astron. Astrophys.* 428, 261–285. <https://doi.org/10.1051/0004-6361:20041335>.
- Lenton, T.M., Held, H., Kriegler, E., Hall, J.W., Lucht, W., Rahmstorf, S., Schellnhuber, H.J., 2008. Tipping elements in the Earth's climate system. *Proc. Natl. Acad. Sci. Unit. States Am.* 105, 1786–1796. <https://doi.org/10.1073/pnas.0705414105>.
- Marwan, N., 2008. A historical review of recurrence plots. *Eur. Phys. J. Spec. Top.* 164, 3–12. <https://doi.org/10.1140/epjst/e2008-00829-1>.
- Marwan, N., 2010. How to avoid potential pitfalls in recurrence plot based data analysis. *J. Biofur. Chaos* 21, 1003–1017. <https://doi.org/10.1142/S0218127411029008>.
- Marwan, N., Romano, M.C., Thiel, M., Kurths, J., 2007. Recurrence plots for the analysis of complex systems. *Phys. Rep.* 438, 237–329. <https://doi.org/10.1016/j.physrep.2006.11.001>.
- Maslin, M.A., Trauth, M.H., 2009. Plio-pleistocene eastern african pulsed climate variability and its influence on early human evolution. In: Grine, F.E., Leakey, R.E., Fleagle, J.G. (Eds.), *The First Humans—Origins of the Genus Homo*. Springer, Vertebrate Paleobiology and Paleoanthropology Series, pp. 151–158. https://doi.org/10.1007/978-1-4020-9980-9_13.
- McDougall, I., Brown, F.H., Fleagle, J.G., 2005. Stratigraphic placement and age of modern humans from Kibish, Ethiopia. *Nature* 433, 733–736. <https://doi.org/10.1038/nature03258>.
- Moore, J.M., Davidson, A., 1978. Rift structure in southern Ethiopia. *Tectonophysics* 46, 159–173. [https://doi.org/10.1016/0040-1951\(78\)90111-7](https://doi.org/10.1016/0040-1951(78)90111-7).
- Nicholson, S.E., 2017. Climate and climatic variability of rainfall over eastern Africa. *Rev. Geophys.* 55, 590–635. <https://doi.org/10.1002/2016RG000544>.
- Ossendorf, G., Groos, A., Bromm, T., Tekelemariam, M.G., Glaser, B., Lesur, J., Schmidt, J., Akçar, N., Bekele, T., Beldados, A., Demissew, S., Kahsay, T.H., Nash, B.P., Nauss, T., Negash, A., Nemomissa, S., Veit, H., Vogelsang, R., Woldu, Z., Zech, W., Oppenorth, L., Miehle, G., 2019. Middle Stone Age foragers resided in high elevations of the glaciated Bale Mountains, Ethiopia. *Science* 365, 583–587. <https://doi.org/10.1126/science.aaw8942>.
- Packard, N.H., Crutchfield, J.P., Farmer, J.D., Shaw, R.S., 1980. Geometry from a time series. *Phys. Rev. Lett.* 45, 712–716. <https://doi.org/10.1103/PhysRevLett.45.712>.
- Potts, R., 1996. Evolution and climate variability. *Science* 273, 922–923. <https://doi.org/10.1126/science.273.5277.922>.
- Potts, R., 2013. Hominin evolution in settings of strong environmental variability. *Quat. Sci. Rev.* 73, 1–13. <https://doi.org/10.1016/j.quascirev.2013.04.003>.
- Roberts, H.M., Bronk Ramsey, C., Chapot, M.S., Deino, A., Lane, C.S., Vidal, C., Vogelsang, R., Cohen, A.S., Lamb, H.R., Asrat, A., Cohen, A., Foerster, V., Lamb,

- H.F., Schaebitz, F., Trauth, M.H. (2021) Using multiple chronometers to establish a long, directly-dated lacustrine record: constraining >600,000 years of environmental change at Chew Bahir, Ethiopia. *Quater. Sci. Rev.*, 10.1016/j.quascirev.2021.107025
- Ravelo, A.C., Andreasen, D.H., Lyle, M., Lyle, A.O., Wara, M.W., 2004. Regional climate shifts caused by gradual global cooling in the Pliocene epoch. *Nature* 429, 263–267. <https://doi.org/10.1038/nature02567>.
- Scerri, E.M.L., et al., 2018. Did our species evolve in subdivided populations across Africa, and why does it matter? *Trends Ecol. Evol.* 33, 592–594. <https://doi.org/10.1016/j.tree.2018.05.005>.
- Schreiber, T., 1993. Extremely simple nonlinear noise-reduction method. *Phys. Rev.* 47, 2401. <https://doi.org/10.1103/PhysRevE.47.2401>.
- Shanahan, T.M., McKay, N.P., Hughen, K.A., Overpeck, J.T., Otto-Bliesner, B., Heil, C.W., King, J., Scholz, C.A., Peck, J., 2015. The time-transgressive termination of the African Humid period. *Nat. Geosci.* 8, 140–144. <https://doi.org/10.1038/ngeo2329>.
- Stringer, C., Galway-Witham, J., 2017. On the origin of our species. *Nature* 546, 212–214. <https://doi.org/10.1038/546212a>.
- Takens, F., 1981. Detecting Strange Attractors in Turbulence. *Lecture Notes in Mathematics*, vol. 898. Springer, Berlin Heidelberg New York, pp. 366–381. <https://doi.org/10.1007/BFb0091924>.
- Tierney, J.E., deMenocal, P.B., 2013. Abrupt shifts in Horn of Africa hydroclimate since the last glacial maximum. *Science* 342, 843–846. <https://doi.org/10.1126/science.1240411>.
- Trauth, M.H., Asrat, A., Duesing, W., Foerster, V., Kraemer, K.H., Marwan, N., Maslin, M.A., Schaebitz, F., 2019. Classifying past climate change in the Chew Bahir basin, southern Ethiopia, using recurrence quantification analysis. *Clim. Dynam.* 53, 2557–2572. <https://doi.org/10.1007/s00382-019-04641-3>.
- Trauth, M.H., Bergner, A.G.N., Foerster, V., Junginger, A., Maslin, M.A., Schaebitz, F., 2015. Episodes of environmental stability and instability in late Cenozoic lake records of Eastern Africa. *J. Hum. Evol.* 87, 21–31. <https://doi.org/10.1016/j.jhevol.2015.03.011>.
- Trauth, M.H., Foerster, V., Junginger, A., Asrat, A., Lamb, H.F., Schaebitz, F., 2018. Abrupt or gradual? Change point analysis of the late Pleistocene-Holocene climate record from Chew Bahir, southern Ethiopia. *Quat. Res.* 90, 321–330. <https://doi.org/10.1017/qua.2018.30>.
- Trauth, M.H., Larrasoana, J.C., Mudelsee, M., 2009. Trends, rhythms and events in Plio-Pleistocene African climate. *Quat. Sci. Rev.* 28, 399–411. <https://doi.org/10.1016/j.quascirev.2008.11.003>.
- Trauth, M.H., Maslin, M.A., Deino, A., Strecker, M.R., 2005. Late cenozoic moisture history of eastern Africa. *Science* 309, 2051–2053. <https://doi.org/10.1016/j.quascirev.2010.07.007>.
- Trauth, M.H., 2013. TURBO2: a MATLAB simulation to study the effects of bioturbation on paleoceanographic time series. *Comput. Geosci.* 61, 1–10. <https://doi.org/10.1016/j.cageo.2013.05.003>.
- Viste, E., Sorteberg, A., 2013. The effect of moisture transport variability on Ethiopian summer precipitation. *Int. J. Climatol.* 33, 3107–3312. <https://doi.org/10.1002/joc.3566>.
- Vogelsang, R., Bubenzer, O., Kehl, M., Meyer, S., Richter, J., Zinaya, B., 2018. When hominins conquered highlands—an acheulean site at 3000 m a.s.l. on mount dendi/Ethiopia. *J. Paleol. Archaeol.* 1, 302–313. <https://doi.org/10.1007/s41982-018-0015-9>.
- Vrba, E.S., 1985. Environment and evolution: alternative causes of the temporal distribution of evolutionary events. *South African J. Sci.* 81, 229–236.
- Vrba, E.S., 1993. Turnover-pulses, the Red Queen, and related topics. *Am. J. Sci.* 293A, 418–452. <https://doi.org/10.2475/ajs.293.A.418>.
- Vrba, E.S., 1995. The fossil record of African antelopes (mammalia, bovidae) in relation to human evolution and paleoclimate. In: Vrba, E.S., Denton, G.H., Partridge, T.C., Burckle, L.H. (Eds.), *Paleoclimate and Evolution, with Emphasis on Human Origins*. Yale University Press, New Haven and London, pp. 385–424.
- Webber, C.L., Zbilut, J.P., 2005. Recurrence quantification analysis of nonlinear dynamical systems. In: Riley, M.A., Van Orden, G.C. (Eds.), *Tutorials in Contemporary Nonlinear Methods for the Behavioral Sciences*. <https://doi.org/10.1007/978-3-319-07155-8>.
- Wessel, P., Smith, W.H.F., 1996. A global self-consistent, hierarchical, high-resolution shoreline Database. *J. Geophys. Res.* 101 (B4), 8741–8743. <https://doi.org/10.1029/96JB00104>.
- Westerhold, T., Marwan, N., Drury, A.J., Liebrand, D., Agnini, C., Anagnostou, E., Barnett, J.S.K., Bohaty, S.M., De Vleeschouwer, D., Florindo, F., Frederichs, T., Hodell, D.A., Holbourn, A.E., Kroon, D., Lauretano, V., Littler, K., Lourens, L.J., Lyle, M., Pälike, H., Röhl, U., Tian, J., Wilkens, R.H., Wilson, P.A., Zachos, J.C., 2020. An astronomically dated record of Earth's climate and its predictability over the last 66 million years. *Science* 369, 1383–1387. <https://doi.org/10.1126/science.aba6853>.
- Zbilut, J.P., Webber Jr., C.L., 1992. Embeddings and delays as derived from quantification of recurrence plots. *Phys. Lett.* 171, 199–203. [https://doi.org/10.1016/0375-9601\(92\)90426-M](https://doi.org/10.1016/0375-9601(92)90426-M).